Understanding the effect of hygroscopic cycling on the internal stress and stiffness of natural fibre biocomposites

V Popineau, A. Celino, M. Peron, C. Baley, A. Le Duigou

Understanding the effect of hygroscopic cycling on the internal stress and stiffness of natural fibre biocomposites

V. Popineau[1], A. Célino[2], M. Péron[2], C. Baley[1] and A. Le Duigou*[1]

1 : Université de Bretagne-Sud, IRDL UMR CNRS 6027, Pole Thématique Composite, Rue Saint-Maudé, BP 92 116, 50321 Lorient Cedex – France

2 : Université de Nantes, GeM, Institut de Recherche en Génie Civil et Mécanique, Equipe E3M 58 rue Michel Ange, BP420, 44600 Saint-Nazaire – France

*Corresponding author: antoine.le-duigou@univ-ubs.fr

Abstract

This article investigates the development and the evolution of hygroscopic stresses within flax/ Polypropylene + Maleic Anhydride grafted Polypropylene (PP+MAPP) asymmetric biocomposites when exposed to various hygroscopic cycles that simulate a wide range of outdoor applications with large Relative Humidity (RH) variation (from 11 to 50% RH, 50-99% RH, 11-99% RH) and with various cycling periods (1-week and 24-hour cycles between 50 and around 90% RH). The transversal and longitudinal tensile properties of biocomposite laminates are characterised, and the weight and curvature of the asymmetric samples are tracked throughout the cycles. The study shows that the hygroscopic cycles entail a reduction of internal stress due to damage development and a relaxation mechanism that are illustrated by permanent hygroscopic deformations. Two parameters have been identified to play a role on the damage development: the magnitude of the RH level and the duration of the cycles.

Keywords: A Natural fibres; A Biocomposites; B Residual stress.

1. Introduction

Natural fibres, including flax fibres, are receiving increased attention in several sectors such as the automotive [1] and marine industries [2], as they exhibit competitive tensile properties combined with low density [3]. Moreover, they are more environmentally attractive than glass fibres as reinforcement for composite materials [4]. However, their moisture-related performance is still not well understood, even though it represents a major limitation to their industrial applicability. Reviewing the related literature shows that most articles deal with their immersion in water and its consequences on mechanical

30 properties. Flax fibres can absorb moisture up to 20% of their mass at 99% relative humidity (RH) [5],
31 which brings their radial swelling up to more than 20% [6]. When they are embedded in a composite and
32 submitted to wet environments, hygroscopic stresses arise due to differential swelling between fibre and
33 matrix [7].
34 For the sake of clarity, residual stresses mostly refer to process-induced stresses [8–11], whereas internal
35 stresses are induced by environmental (moisture content [12], temperature [13]) or mechanical loading
36 [14, 15]. For a single flax fibre, the Coefficient of Hygroscopic Expansion (CHE) in the radial direction
37 has been estimated to be $\beta_T = 1.14\ \varepsilon/\Delta C$ [6] and to lead to much superior strains than those induced by
38 their Coefficient of Thermal Expansion (CTE0 ($\alpha_{fT} = 83\ 10^{-6}\ \varepsilon/°C$ [16]). The axial direction undergoes
39 weak expansion due to the low cellulose microfibril angle in the S2 layer of flax fibres [17]. The
40 hygroscopic internal stresses can induce micro-cracking of the matrix [18], influence the moisture uptake
41 [19], and finally alter the mechanical performance [7, 20-21]. Some work has indicated that a
42 compressive state around the fibres may however enhance the load transfer properties [6]. It is thus
43 necessary to better understand the generation of hygroscopic stresses on a biocomposite system.
44 To this end, several authors [22,23] have shown that it is possible to estimate the transverse stress state of
45 [0°, 90°, 0°] symmetric laminates by measuring the curvature of a [0°, 90°] asymmetric laminate of the
46 same material. Very few studies deal with natural fibre-reinforced biocomposites. Péron et al. [7, 12] have
47 used flax/PP+MAPP asymmetric laminates exposed to immersion or relative humidity and compared the
48 experimentally measured curvature with the numerically predicted one. This produced good agreement
49 that permitted the validation of the numerical model. These asymmetrical configurations can also be used
50 to develop new paradigmatic smart materials, i.e., shape-changing hygromorph biocomposites [24–29].
51 During their life cycle in outdoor applications, biocomposites are rarely exposed to a unique
52 environmental condition but may be subjected to environmental cycling. To the best of the authors'
53 knowledge, no available article deals with the impact of environmental cycling on the behaviour of
54 asymmetric biocomposites to better understand the evolution of the induced stress state.
55 All the available articles focus on symmetric biocomposites subjected to water immersion and drying
56 cycles [27, 30–34]. Some authors have used immersion and drying times as key variables for their
57 experiments (i.e., "transient" cycles) while others have waited for stabilization in the mass of their
58 samples (i.e., "saturation" cycles). A few studies have focused on the hygrothermal cycling of

biocomposites in water vapour environments [35-37]. Moreover, no clear justification has been proposed for the selection of the hygroscopic conditions despite its necessity for the analysis of results.

Hence, the present article aims to fill the gap with regard to understanding the generation and evolution of hygroscopic internal stresses in a biocomposite during hygroscopic cycles that simulate a wide range of outdoor applications. The resulting typology and effects are discussed, and the establishment of an original scenario is proposed.

For the study, asymmetric flax/PP+MAPP biocomposite stripes were manufactured by Vacuum-Bag-Only (VBO) moulding, along with longitudinal and transversal tensile samples. The samples were exposed to different hygroscopic cycles. First, "saturation" hygroscopic cycles were performed, where the change in condition was triggered by the stabilization in weight of the samples achieved at 23 °C, under three different environmental conditions. In parallel, "transient" hygroscopic cycles were applied with a cycling period of 1-week cycles and 24-hour cycles. The moisture content and curvature of the asymmetric samples were tracked along the hygroscopic cycles. In addition, the unidirectional samples gave access to the hygroexpansion, tensile longitudinal and transversal stiffnesses of the biocomposites throughout the cycles. Finally, an estimation of the stress state in an equivalent symmetric lay-up was calculated.

2. Material and methods

2.1. *Materials, manufacturing route, and samples used*

For the processing of the biocomposites, 50 g/m² unidirectional flax tapes were supplied by Linéo – NatUp (Flaxtape FT50). According to the manufacturer, no physical or chemical treatment was carried out on the fibres, which were harvested in France, dew retted, scutched, and hackled. Polypropylene (PP) (Total Petrochemicals PPC 3660) and compatibilized PP with 4% Maleic Anhydride (MAPP) (Arkema Orevac CA 100) were mixed and extruded as films.

The biocomposites were processed with film stacking and VBO moulding. FT50 tapes (12 plies) and PP+MAPP films were stacked on an aluminium plate with a caul plate to reduce thickness variation. Spacers were used to control the final thickness of the part. A draining fabric was settled around the lay-up, and the vacuum-bag was then sealed. Based on a previous parametric study [2], the whole set up was placed in an oven at 180°C during 45 min and vacuumed at 950 mbar. The fibre volume fraction was targeted to be 40%. By controlling the number of polymer films, density measurement estimated a fibre

volume fraction of 42.2 ± 1.5%. The densities of the PP+MAPP and related flax-reinforced biocomposites were measured by immersion method in ethanol, as described in ISO 1183, on at least five samples of each, using a Mettler Toledo MS-DNY-54 balance (accuracy 10^{-4} g). The density of the dried flax fibres was measured with an AccuPyc II 1340 gas pycnometer from Micromeritics™, using helium. The density of the matrices was found to be 0.90 ± 0.01 for the PP+MAPP and 1.14 ± 0.00 for the Epoxy resin. The density of the dried flax fibres was 1.48 ± 0.02.

Two thermocouples recording the temperatures during the process were placed in the centre of the oven and in the middle of one stack. The thermal cycle applied in the oven was composed of a heating step at 10°C/min, a plateau at the processing temperature, and a cooling step. The cooling rate was around 1°C/min due to the oven thermal inertia and air-cooling process.

The selected process enabled the manufacturing of thermoplastic composite parts with potentially large dimensions and complex shapes. The materials were stored at 23°C, 50% RH several weeks before processing until their weight was constant.

The $[0°]_{12}$ unidirectional flax/PP+MAPP plates were processed and cut into 250mm-long and 15mm-wide stripes for the longitudinal samples and 250mm-long and 25mm-wide stripes for the transversal tensile samples, using a milling machine. Those samples were then equipped with $[\pm 45]_S$ glass/epoxy tabs as grip areas. $[0°_3; 90°_9]$ asymmetric flax/PP+MAPP plates were processed and cut into 10 x 70mm stripes in order to study the development of residual and internal stresses within the biocomposites [27]. This stacking sequence was chosen to maximise the amplitude of curvature, using the Timoshenko equations [13] for slender beam structures, such as described in [27].

2.2. *Environmental conditions, "saturation" and "transient" hygroscopic cycles*

A laboratory conditioned at 23°C, 50% RH was used for the conditioning of the materials prior to processing and of the biocomposites prior to testing. These conditions of 23°C, 50% RH constitute the reference state at which there is no environmental loading. To study the development and evolution of the hygroscopic stresses through hygroscopic cycles, different types of cycles were examined, such as schematised in Fig. 1.

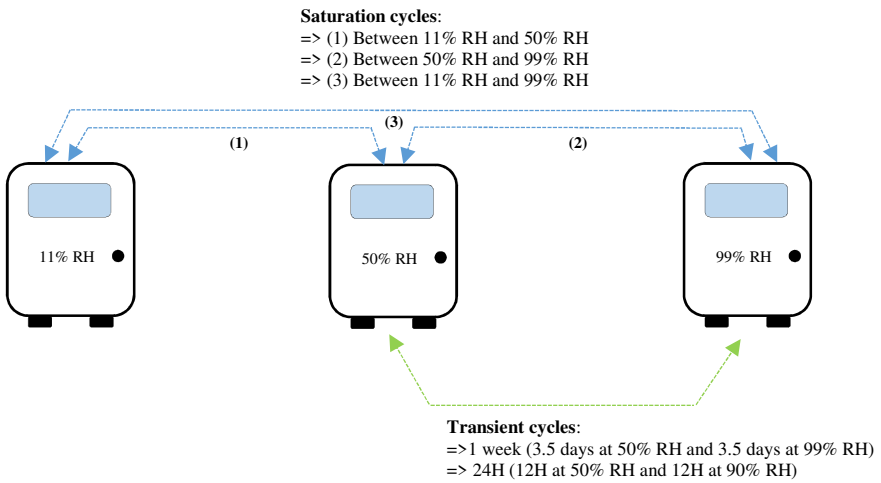

Fig. 1 – Schematisation of the various typologies of hygroscopic cycles examined in this work. Blue dotted lines: Hygroscopic cycles are achieved until saturation at 23°C between 11 and 50% RH, 50 and 99% RH, and 11 and 99% RH. Saturation times are variable. Green dotted lines: Transient hygroscopic cycles with fixed cycle periods are also examined: 1-week cycles between 50 (3.5 days) and 99% RH (3.5 days) and 24-hour cycles between 50 (12H) and 90% RH (12H). Moisture content is variable.

During the "saturation" cycles, the samples were conditioned in hermetic tanks at laboratory temperature at $23.2 \pm 2.2\ °C$, in which the relative humidity was controlled using saturated salt solutions. Throughout the different cycles, saturation was reached with a mean period of 12 days. The salts used were potassium hydroxide, magnesium nitrate, and potassium sulphate. Three different "saturation" cycles were examined in those tanks: between 11 and 50% RH, between 50 and 99% RH, and between 11 and 99% RH.

The environmental conditions (variation in time and RH) applied in this experiment did not follow any industrial standards where the humidity range is often prescribed. The purpose of the test was to bring fundamental information on the effect of the largest typologies of the humidity cycles (time and delta RH). In consequence, the results produced can be applied to a larger range of outdoor applications. In the literature, 50% RH is considered as the most well-established humidity condition used. In this regard, it is often included in the standard of mechanical characterization and enables better comparisons. The purpose of selecting 11 and 99% was to evaluate the effect of dry and wet environments that may be found in extreme outdoor environments. The salted solution induced the value of RH for a fixed temperature in order to evaluate the effect of the moisture content variation using the hypothesis of moisture being homogeneously distributed in the material. This hypothesis did not match practical outdoor applications where RH variation and consequently moisture variation are quicker and prevent

materials from reaching saturation. However, this choice constituted an ideal case deemed to facilitate fundamental understanding of hygroscopic stress generation through calculations with reduced uncertainties.

One batch of 7 asymmetric stripes, 12 longitudinal tensile and 12 transversal tensile samples was assembled per cycling condition. The mass of the asymmetric stripes was measured daily for every condition. When stabilization was reached after five weightings in the same range (i.e., five consecutive values with no variation), the batches were moved to the next condition. Four longitudinal and four transversal tensile samples were picked up after 1, 3, and 7 "saturation" cycles to be measured and tested. Two "transient" cycles were examined, during which the period of cycling was kept constant. Samples were exposed to 30 hygroscopic cycles in the hermetic tanks with saturated salt solutions between 50 and 99% RH with a cycling period of 1 week (3.5 days per condition). To study a shorter period of cycling, a humidity chamber (Memmert HCP) was used for practical reasons. A 24-hour cycle was achieved (12 hours per condition) between 50 and 90% RH, at 23°C, as 90% RH constitutes the limit of the machine. A 24-hour transient cycle corresponds to moisture variation at the day level. The aim was to bring information closer to outdoor applications. However, the results are more complex to interpret due to the heterogeneous distribution of moisture within the sample and the additional stresses that it generates [12]. A 1-week cycle is considered as very close to the saturation cycle, which is finally the upper bound of the transient cycles.

One batch of 7 asymmetric stripes, 15 longitudinal and 15 transversal samples was assembled per "transient" cycling condition. At least three longitudinal and transversal tensile samples were picked up after 3, 10, 21, and 30 cycles for the 1-week cycles, and 10, 25, 52, and 103 cycles for the 24-hour cycles.

2.3. *Gravimetric measurements*

The weighing was performed using a Mettler Toledo MS-DNY-54 balance (accuracy 10^{-4} g). The dry mass of the flax/PP+ MAPP biocomposites was determined by drying a batch of five native samples with vacuum at 105°C during 72 h [2, 39]. From that dry mass m_0, supposing that the change in mass of the samples was only due to the sorption of water by the biocomposites, the moisture content ($\%MC$) was tracked in the samples by weighing them, hence giving access to their mass m, using Equation 1:

$$\%MC = \frac{(m-m_0)}{m_0} * 100 \qquad \text{Eq. 1}$$

178 The moisture content of the samples was calculated in the "saturation" cycles from the fifth stabilised
179 weight measurement in every condition, just before the tank switch. During the "transient" cycles, the
180 asymmetric samples were regularly picked up just before the switch in condition, and their weight and
181 curvature were measured.

182 ### 2.4. *Curvature measurements*

183 The curvature of the asymmetric samples, as shown in Fig. 2b, was measured to access the development
184 of residual and internal hygroscopic stresses within the biocomposites. The inside outline of the bent
185 beams and samples was drawn on a paper sheet, scanned, and processed with the image analysis software
186 ImageJ® (National Institutes of Health, USA). A "circle fit" function can measure the bending curvature
187 (κ) of the samples, as shown in Fig. 2b. A null curvature $\kappa = 0$ corresponds to an infinite radius, and thus
188 to a flat sample. By convention, the curvature is considered negative $\kappa < 0$ when the sample is bent such
189 as the [90°] layer is inside the circle and positive $\kappa > 0$ when it is outside the circle.
190 The curvature of the samples at dry state was measured just after being removed from the oven. The
191 materials were considered dried, and the hypothesis was that the bending was induced only by the
192 residual thermal stresses induced by the manufacturing route. The samples were then stored until
193 stabilization at 23°C, 50% RH. The curvature measured at that point gave access to the sum of the
194 thermal and hygroscopic residual stresses in the material σ_R.
195 The curvature of the asymmetric samples exposed to "saturation" cycles was measured at stabilization in
196 every condition before the tank switch. The curvature of the asymmetric samples exposed to "transient"
197 cycles was measured regularly, as mentioned in the previous section, along with the weight measurement.
198

199 ### 2.5. *Tensile stiffness and swelling measurements*

200 Mechanical tests were carried out to access the evolution of the longitudinal and transversal moduli of the
201 flax/PP+MAPP biocomposites across the cycles to calculate the transversal internal stresses across the
202 hygroscopic cycles. Mechanical tensile tests were performed in the laboratory at 23°C, 50% RH, in
203 accordance with ISO 527-5. The loading speed was 1 mm/min. The monotonic tensile tests were carried
204 out using an electromechanical MTS Criterion Model 42 test machine, fitted with a 5 kN load cell and an
205 MTS extensometer with a gauge length of 25 mm. For the longitudinal tests, the initial tensile modulus E_1
206 was calculated between 0.025% and 0.1% of strain and the second tensile modulus E_2 after 0.4% of strain,

as recommended in the literature [40]. For the transversal tests, the transversal modulus E_T was calculated from 0.05 to 0.25% of strain, as specified by ISO 527-1.

One set of 4 longitudinal and 4 transversal samples was tested without being exposed to any hygroscopic cycles after stabilization at 23°C, 50% RH. The tensile samples mentioned in section 2.2 were tested after being exposed to a certain number of hygroscopic cycles and after being conditioned until stabilization at 23°C, 50% RH, for both "saturation" and "transient" cycles.

The dimensions of the longitudinal and transversal tensile samples were measured in the in-plane and out-of-plane directions using a Mitutoyo micrometre with a 10^{-3} mm accuracy. Those measurements were performed before any hygroscopic cycling, after stabilization at 23°C, 50% RH, and after the chosen number of cycles and stabilization at 23°C, 50% RH. These measurements were used to calculate the permanent swelling deformations in the longitudinal, transversal, and out-of-plane directions of the biocomposites, with Equation 2:

$$\Delta x = \frac{(x - x_{BC})}{x_{BC}} \qquad \text{Eq. 2}$$

x being a dimension measurement in a given direction and x_{BC} the measurement in the same direction before any cycle is done.

2.6. *Calculation of the stress state in the equivalent symmetric lay-up*

As mentioned earlier, and shown by several authors [9, 13, 22], it is possible to calculate the total stress state σ_{TOTAL}, which is the sum of residual and internal stresses of the [90°] layer of a [0°, 90°, 0°] laminate, with the measurements of the curvature of an equivalent [0°, 90°] laminate, made with similar materials, and knowing the longitudinal and transversal stiffness of the unidirectional composite. It is expressed in Equation 3:

$$\sigma_{TOTAL} = -\frac{E_T E_1 k}{E_1 k + E_T h}\left(\frac{b+d}{2} + \frac{(E_1 b^3 + E_T d^3)}{6(b+d)}\left[\frac{1}{E_1 b} + \frac{1}{E_T d}\right]\right) * \kappa \qquad \text{Eq. 3}$$

with E_1 and E_T representing respectively the longitudinal and transversal stiffness of the [0°] layer, k the thickness of both [0°] layers in the symmetric laminate, $2h$ the thickness of the [90°] layer, b and d respectively the thicknesses of the [0°] and [90°] layers in the asymmetric laminate, and κ the curvature of the composite such as described earlier. As shown in Fig. 2, in this work, k and h are respectively considered equal to b and d.

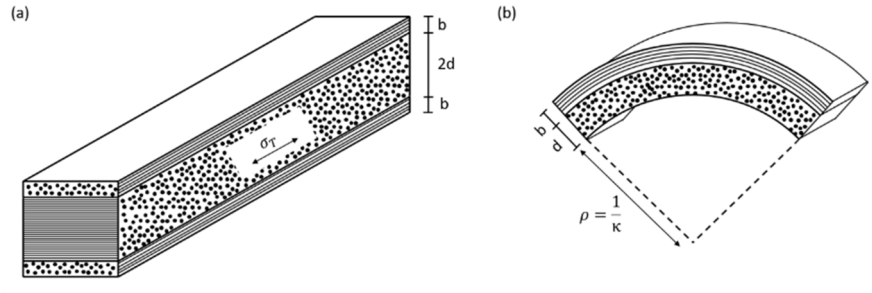

Fig. 2 - Equivalent (a) [0°, 90°,0°] symmetric and (b) [0°, 90°] laminates (*b* and *d* are respectively the thicknesses of the [0°] and [90°] plies).

After calculating the residual stresses σ_{RES} based on post-processing conditions (i.e., dry state) it was possible to evaluate the internal stresses across the cycles σ_{INT}, using Equation 4:

$$\sigma_{INT} = -\frac{E_T E_1 b}{E_1 b + E_T d}\left(\frac{b+d}{2} + \frac{(E_1 b^3 + E_T d^3)}{6(b+d)}\left[\frac{1}{E_1 b} + \frac{1}{E_T d}\right]\right) * \kappa - \sigma_{RES} \qquad \text{Eq. 4}$$

2.7. *SEM observations*

To observe the development of the damage across the cycles, samples were embedded in epoxy resin and polished with a 4000 abrasive sandpaper for observation under a Zeiss, EVO ® 40 scanning electron microscope (SEM).

3. Results and discussion

3.1. *Hygroscopic cycles in saturation conditions*

3.1.1 Moisture content evolution across the "saturation" cycles

The moisture contents at stabilization across the cycles of the flax/PP+MAPP biocomposite asymmetric samples subjected to «saturation» cycles are presented in Fig. 3a and b.

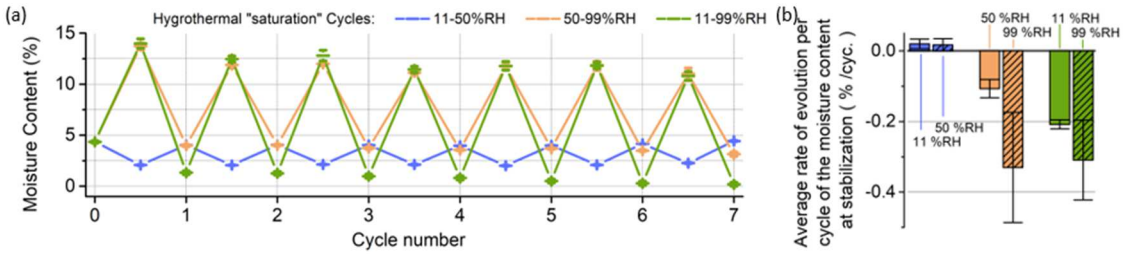

Fig. 3 – (a) Moisture content of the flax/PP+MAPP asymmetric samples across the different "saturation" hygroscopic cycles. (b) Mean rate of evolution per cycle of the moisture content of the flax/PP+MAPP asymmetric samples across the different "saturation" hygroscopic cycles.

The first point at the cycle N.0 corresponds to the stabilization of the samples at 23°C, 50% RH after manufacturing. The initial moisture content is 4.10 ± 0.12 at 23°C, 50% RH, 2.12± 0.05% at 23°C, 11% RH, and 13.74± 0.16% at 23°C, 99% RH.

Fig. 3b shows the rate of evolution of the moisture content at saturation for the flax/PP+MAPP samples exposed to the different hygroscopic "saturation" cycles. We first note that the moisture content at saturation of the flax/PP+MAPP samples exposed to hygroscopic cycles between 11 and 50% RH is almost constant across the cycles. After seven cycles, the moisture content is 4.09 ± 0.16 at 50% RH and 2.10 ± 0.07 at 11% RH. The average moisture contents of the upper and lower boundaries are respectively 2.11 ± 0.07% at 23 °C, 11% RH and 4.09 ± 0.15% at 23 °C, 50% RH.

Regarding the samples with larger hygroscopic amplitudes, i.e., "saturation" cycles between 50 and 99% RH and between 11 and 99% RH, the moisture contents at saturation show a decrease across the cycles (Fig. 3b). The final moisture content, after seven cycles between 50 and 99% RH, is 3.3 ± 0.11 % at 23°C, 50% RH and 11.60 ± 0.16% at 23 °C, 99% RH.

Samples exposed to larger cycles between 11 and 99% RH show a relatively greater decrease in both boundary conditions than the samples exposed to cycles between 50 and 99% RH. The final moisture content, after seven cycles between 11 and 99% RH, is close to zero at 23°C 11% RH, 2.71 ± 0.10% at 23°C, 50% RH and 11.52 ± 0.17% at 23 °C, 99% RH. Péron et al. [12] have shown that when a biocomposite material is exposed successively to different environments, the greater the difference in relative humidity between the two environments, the greater the transient internal stresses that the material endures. Those stresses might be relaxed in the matrix, as shown by Newman et al. [33], inducing the creation of a gap between the fibre and the matrix when the fibre shrinks again, and thus accelerating the water damages.

Newman et al. [33], using epoxy/flax composites during 12 immersion/drying cycles, have shown that the moisture content was slightly increased. Opposite results have been found by [17, 41, 42] where loss of mass in immersion was observed during immersion/drying cycles and stated to be the result of soluble polysaccharide leaching.

Nonetheless, the hygroscopic cycles examined here do not involve an immersion test, and the water is present only in its vapour state. Cadu et al. [35] observed such a decrease in mass across hygroscopic cycles and explained it as caused by hornification phenomena. When a certain level of water is removed from the flax fibres, there is a microstructural change such as pore closure, and the hydrogen bonds that link the polysaccharides together are broken and rebuilt within the molecules, inducing a loss of available hydroxyl groups and thus a loss in hydrophilicity [43][44]. However, the decrease in mass is so important that the samples exposed to cycles between 11 and 99% RH show a mass at stabilization at 11% RH at the seventh cycle that is in the same order of magnitude as the dry mass of the samples, measured after drying under vacuum at 105°C during 72 hours, close to 0%. Thus, hornification may not be the only explanation for this observation.

This loss of dry mass during hygroscopic cycles may be explained by other mechanisms such as the triggering of micro-organisms activity, such as bacteria and fungus, naturally existing in natural fibres [45]. This point deserves to be further investigated elsewhere. As shown in Fig. 4, after 15 days of exposition to 99% RH, fungal activity such as mold, whose growth might have consumed the organic substract, appears at the surface of the flax/PP+MAPP samples.

Fig. 4 - Pictures of the surface of flax/PP+MAPP asymmetric samples after conditioning 15 days at 99 %RH. The red circle highlights the appearance of mold.

3.1.2 Permanent out-of-plane swelling deformations across the "saturation" cycles

The permanent hygroscopic deformations measured on the longitudinal and transversal samples across the "saturation" hygroscopic cycles are presented in the in-plane longitudinal and transversal directions and in the out-of-plane direction in Fig. 5a, b, and c, respectively.

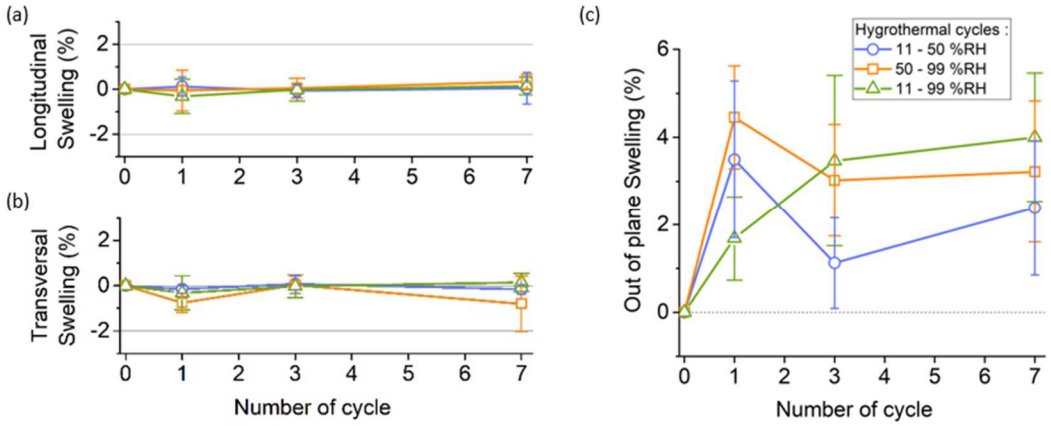

Fig. 5 – Permanent swelling in the (a) longitudinal, (b) transversal, and (c) out-of-plane direction of flax/PP+MAPP biocomposite unidirectional samples across different "saturation" cycles.

No permanent deformations are observed in the in-plane longitudinal and transversal directions across the "saturation" cycles (Fig. 5a and b). Although the biocomposites are supposed to be transversally isotropic, the swelling behaviour in the transversal and out-of-plane directions are very different (Fig. 5b and c). This point is discussed elsewhere [46] and is proposed to be due to residual stresses implied by the manufacturing route. The permanent deformations in the out-of-plane direction are in the same order of magnitude, regardless of the "saturation" cycle the biocomposite samples were exposed to, around 3%. Similar observations on flax/epoxy samples were made after one cycle of immersion until saturation [42]. The authors explained the trend by the stress release implied by molecular relaxation processes in the matrix. As shown by the SEM observations in Fig. 6, cracks appear at the fibre/matrix interface and fibre/fibre interface during the hygroscopic cycles. This is due to the shrunken fibres that pull away from the matrix and from one another within the bundles.

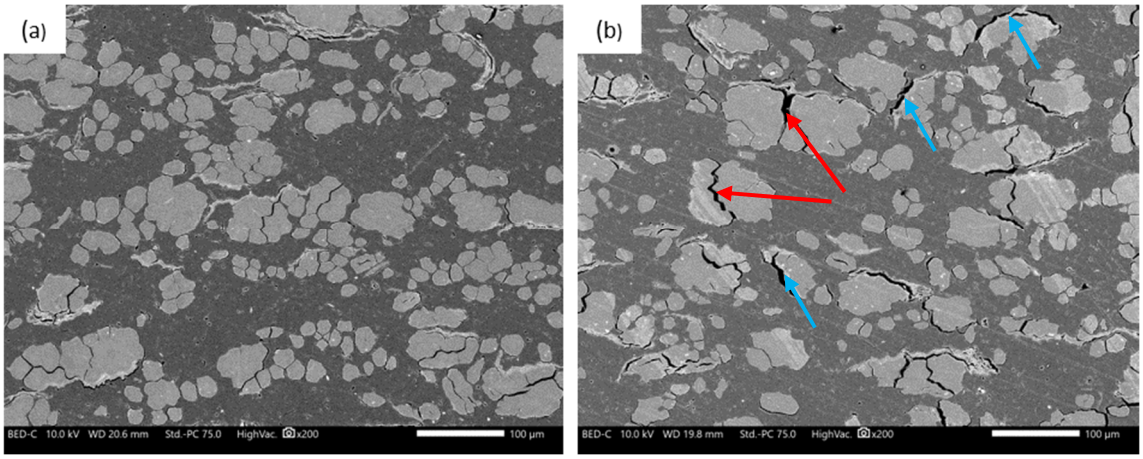

Fig. 6 - SEM observations of cross-sections of flax/PP+MAPP biocomposites laminates, (a) native and (b) after 15 "saturation" cycles between 50 and 99 %RH. Red arrows show intra-bundle cracks while blue arrows show interfacial cracks between fibre and matrix.

Furthermore, the porosity content was observed to increase on flax/epoxy and flax/PP+MAPP composites with immersion cycles [27, 41]. As previously shown [2], the evolution of the porosity content is inversely proportional to the material density. Thus, out-of-plane swelling (Fig. 5) linked with a constant or decreasing mass (Fig. 3) results in a decrease in density. Therefore, it is possible to conclude that the porosity contents in the flax/PP+MAPP samples increase regardless of the "saturation" cycle the biocomposite samples were exposed to.

3.1.3 Longitudinal and transversal stiffness across the "saturation" cycles

The flax/PP+MAPP biocomposite tensile samples tested after exposition to "saturation" cycles all showed typical non-linear behaviours in longitudinal and transversal directions, as described in [2]. No observable difference in behaviour was noticed during hygroscopic cycles. Fig. 7 shows the evolution of the longitudinal and transversal stiffness of the flax/PP+MAPP samples measured at stabilization at 23°C, 50% RH on unidirectional tensile samples that were previously exposed to different "saturation" hygroscopic cycles.

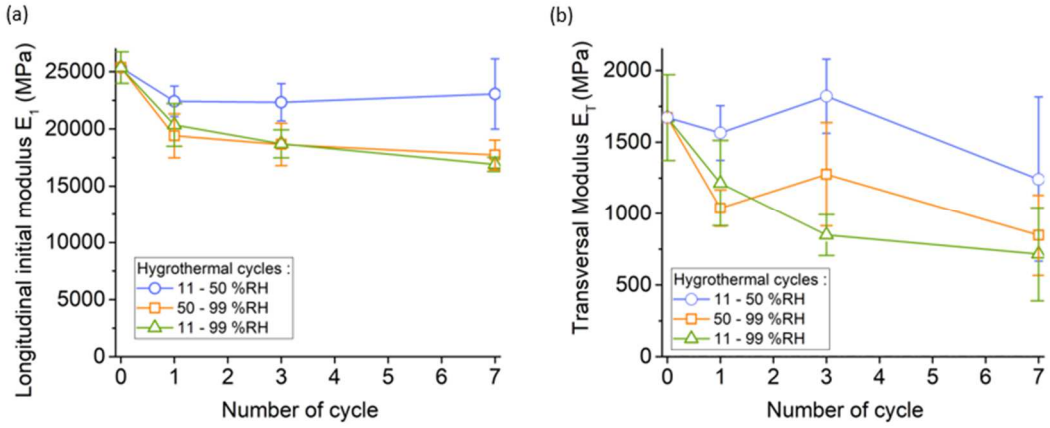

353

354 **Fig. 7 – Longitudinal stiffness E_1 and transversal stiffness E_T of the flax/PP+MAPP unidirectional**
355 **biocomposites measured at 23°C, 50% RH, after exposition to the "saturation" hygroscopic cycles.**

356

357 A decrease in stiffness is observed in both directions for every sample exposed to "saturation"
358 hygroscopic cycles. However, the decay in stiffness for the samples exposed to the hygroscopic cycles
359 between 11 and 50% RH is lower than in the other conditions. After seven "saturation" cycles between 11
360 and 50 RH, which represents about 6 months of cycling, an encouraging drop of only 9% is observed in
361 longitudinal stiffness and 26% in transversal stiffness.
362 Such constancy in dry conditions is not observed when the samples are cycled at higher relative humidity.
363 Samples exposed to "saturation" hygroscopic cycles between 50 and 99% RH and between 11 and 99%
364 RH show decay in longitudinal and transversal stiffness, in the same order of magnitude, with
365 respectively about 30% and 50% of decay. Decays in mechanical characteristics were already observed
366 on flax/epoxy unidirectional biocomposites with 47% V_f exposed to "transient" hygroscopic cycles at
367 55°C, between 40 and 90% RH in both longitudinal [35] and transversal directions [36], with respectively
368 10% and 50%. The trend observed by the authors is slightly different due to the transient state of moisture
369 content within their sample, the lower initial porosity content (Vp =2.5% against 1.9<Vp<8% here [2])
370 and the epoxy matrix that allows better interfacial shear strength with flax fibres than PP+MAPP.

371 *3.1.4 Curvature at stabilization across the "saturation" cycles and calculation of the stress state*
372 During the process of VBO moulding, when the matrix is melted around the flax fibres, just before the
373 cooling sequence, the flax fibres are totally dried [2], and the material is free of any stress [8]. Once the
374 melting temperature is passed, the matrix solidifies around the fibres, and because of their different
375 Coefficient of Thermal Expansion, the unidirectional plies shrink in the transversal and the out-of-plane

directions mostly. Thermal residual stresses develop at the laminate scale for laminate biocomposites, and the asymmetric samples bend once demoulded, with the transversal direction inside. The curvature of the asymmetric flax/PP+MAPP samples at dry state is measured at $-1.2\ 10^{-2} \pm 0.1\ 10^{-2}\ mm^{-1}$. It has been shown that the stiffness of biocomposites is sensitive to their moisture content [17]. However, in the first approximation, the stiffness in longitudinal and transversal directions of the flax/PP+MAPP samples examined is considered equal to those measured at 23°C, 50% RH. With the hypothesis that the curvature at dry state is attributable only to the residual thermal stresses, Eq. 3 enables calculating the latter in the transversal direction of the equivalent symmetric laminate [90°] layer at $12.9\ MPa$. This stress is induced by the transversal shrinking that is restrained by the longitudinal layer. This value is higher than the tensile transversal strength of the composites, measured at $8.9\ MPa$ in a previous work on similar material but with differently shaped samples [2]. It may be a source of irreversible damage, such as found in the SEM observations shown in Fig. 6.

Once exposed to a humid environment, the flax fibres start to swell, while the PP+MAPP matrix is relatively insensitive to the presence of water. The swelling of the fibres induces the expansion of the unidirectional ply, mainly in the transversal and out-of-plane direction, because of the anisotropy of the flax fibres. The swelling of the transversal plies induces a bending of the samples with the transversal ply on the outside. After stabilization at reference state at 23°C, 50% RH, before cycling, the curvature of the asymmetric samples is measured at $-4.5\ 10^{-4} \pm 3.8\ 10^{-5}\ mm^{-1}$, which leads to the estimation of the residual stresses at $\sigma_R = 0.5\ MPa$. This shows that the hygroscopic residual stresses (considering that the sorption up to 50% RH is included in the process) at the reference state almost offset the residual thermal stresses, inducing a null bending moment.

Fig. 8a presents the curvature at stabilization at the different cycling conditions κ, for the biocomposite samples exposed to "saturation" hygroscopic cycles at 23°C, between 11-50% RH, 50-99% RH and between 11-99% RH, across the first seven cycles.

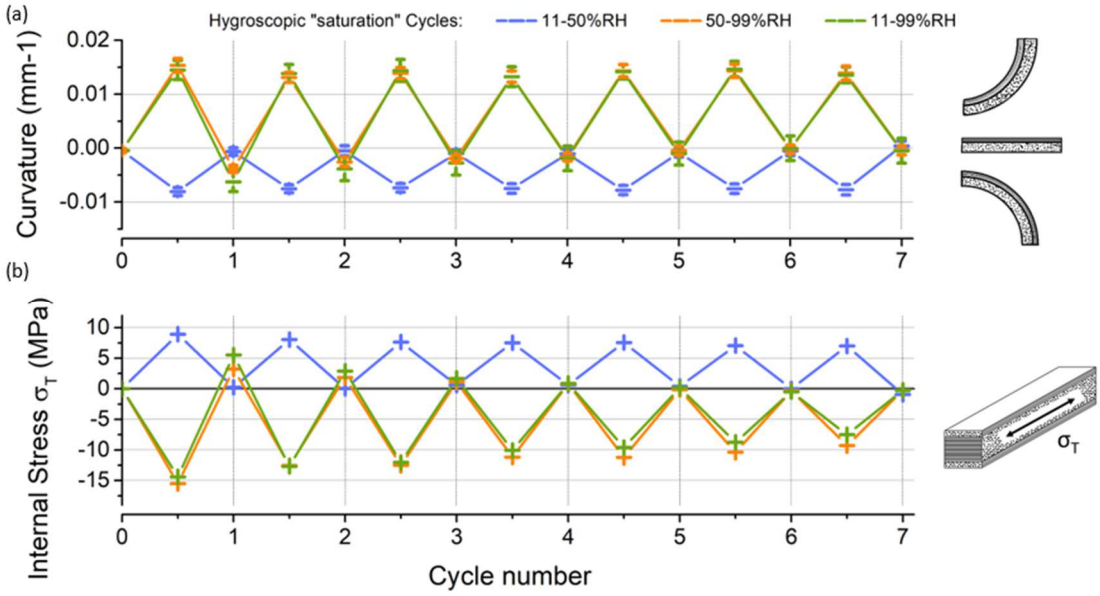

Fig. 8 - (a) Curvatures at stabilization of the flax/PP+MAPP asymmetric biocomposite samples across the "saturation" hygroscopic cycles. (b) Internal stress calculated in the equivalent symmetric laminate [90°] layer across the cycles for the flax/PP+MAPP asymmetric biocomposites exposed to "saturation" cycles.

From these curvatures and linear regressions of the longitudinal and transversal moduli across the cycles(see the Appendix), it is possible to calculate the internal hygroscopic stresses in the equivalent symmetric laminate across the cycles, as shown in Fig. 8b. This is done using Eq. 4 and the hypothesis that the moduli at a given cycle are the same at stabilization at 11, 50 and 99% RH.

This is explained by the swelling in the transversal direction restrained by the [0°] layer, as was also shown by Péron et al. [12]. In the samples subjected to cycles between 11 and 50% RH, internal stresses remain close to 0 MPa at saturation at 50% RH. Internal stresses at saturation at 11% RH decrease from 8.9 MPa to 6.1 MPa across the seven cycles. These stresses remain in the same order of magnitude as the transversal strength, as mentioned before, which may explain the permanent out-of-plane deformations developed across the cycles.

Regarding the samples exposed to cycles between 50 and 99% RH and after one stabilization at 99% RH, the internal stress in the [90°] ply at 50% RH is tensile and calculated at 3.3 MPa, whereas it was expected to be close to 0 MPa, such as in the case of the cycles between 11 and 50% RH. This overreaction of the internal stress response is also observed in the negative curvature of the samples back at 50% RH, and in the literature on flax/PP+MAPP asymmetric laminates [17] and on wood bilayers [47].

The tensile internal stresses calculated in the cycles from 50 and 99% RH and 11 to 99% RH are reduced over the seven cycles, respectively from 3.3 to $-0.3\ MPa$ and from 5.5 to $-0.8\ MPa$. Regarding the compressive stresses at saturation at high moisture content for the cycles between 50 and 99% RH and from 11 to 99% RH, they also exhibit a reduction, respectively from -15.5 to $-9.1\ MPa$ and from -14.4 to $-6.2\ MPa$ (Fig. 8).

When the biocomposites are successively exposed to low relative humidity, their transversal directions are exposed to cycled tensile internal stresses. Those successive internal tensile stresses induce progressive damage in the material, shown by the slight reduction of the mechanical properties (Fig. 7a and b) and the increase of the permanent out-of-plane direction (Fig. 5a, b and c), as schematized in Fig. 9. Those phenomena induce relaxation of the internal hygroscopic stresses across the cycles.

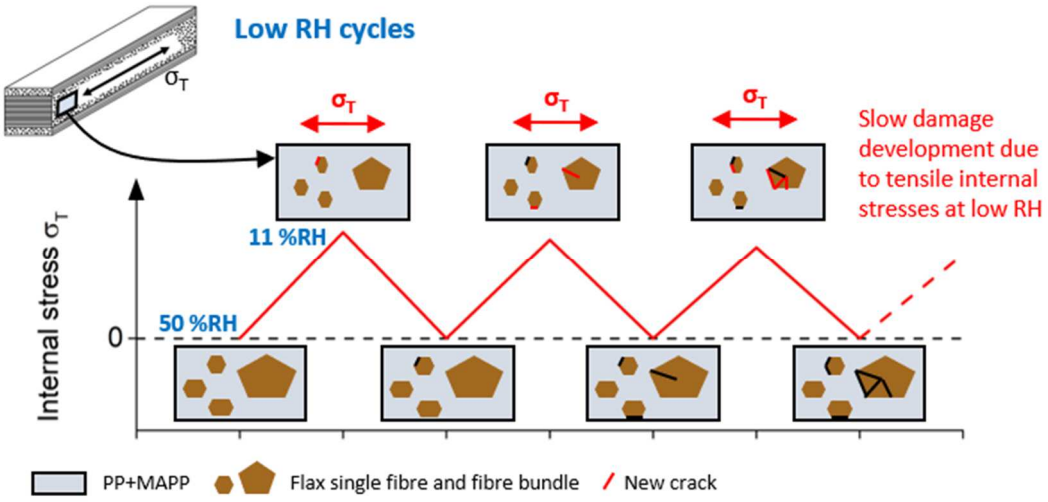

Fig. 9 – Internal stress evolution during successive low RH exposure.

When the samples are exposed to cycles with higher relative humidity, modification of moisture content, reduction of tensile properties, permanent out-of-plane expansion, and change of curvature are shown to be more drastic. Several authors have already shown the effect of swollen flax fibres at high moisture content, promoting irreversible damage such as plastic thresholds overreached in the matrix, leading to micro-cracks [30], cracks within the fibres [32], or viscous relaxation of the stresses within the matrix [33], the fibres, or at the different interfaces (cell-wall, fibre/fibre, and fibre/matrix), as schematized in Fig. 10.

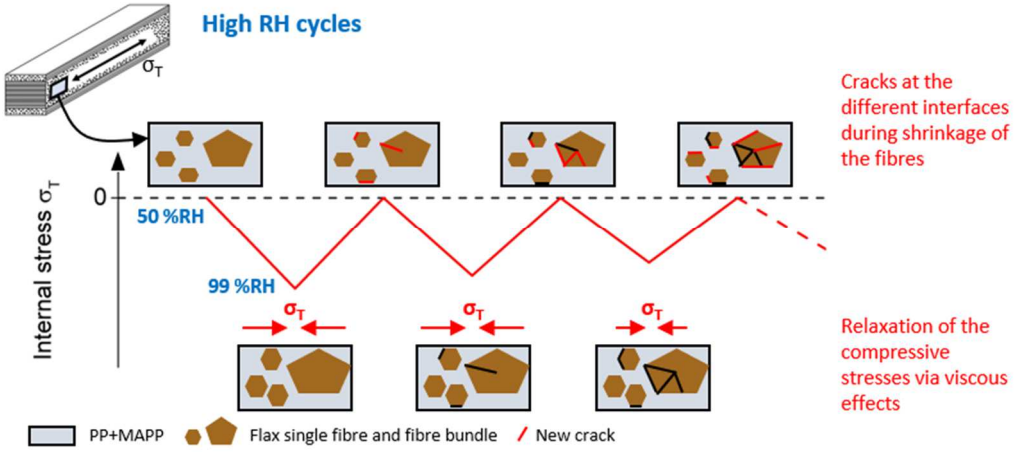

Fig. 10 – Internal stress evolution during successive high RH exposure.

In addition, asymmetric lay-up curvature evolutions during hygroscopic cycles have all shown a reduction through a relaxation process of internal stresses, which is a function of the moisture content gradient. Therefore, a larger moisture content gradient implies a larger relaxation through the plastic matrix deformation in the interface area.

3.2. *"Transient" hygroscopic cycles*

3.2.1 Moisture content across the "transient" cycles

The moisture contents at the end of the cycles of the flax/PP+MAPP samples subjected to "transient" cycles between 50 and 90% RH with a 24-hour period of cycling and with a 1-week period of cycling are presented in Fig. 11. For comparison, the results from the "saturation" cycles between 50 and 99% RH are also presented in Fig. 11.

The moisture content reached at 99% RH by the samples exposed to 1-week cycles is in the same range as the "saturation" samples at the same relative humidity. This shows that after 3.5 days of exposure at 99% RH, saturation is almost reached.

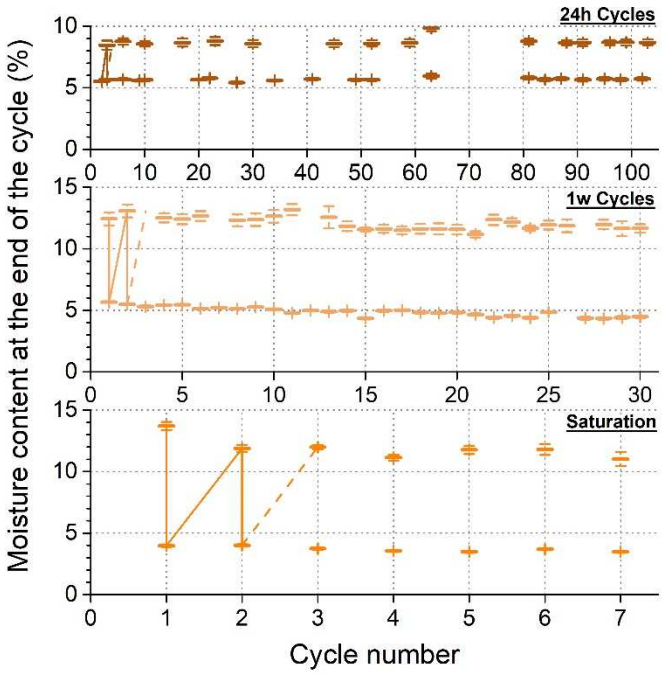

458

459 **Fig. 11 – Mass measurements for the flax/PP+MAPP samples across the different "transient" hygroscopic**
460 **cycles. 103x 24-hour cycles, 30x 1-week cycles, and 7x "saturation" cycles between 50 and 90% RH are presented.**

461

462 A decrease in mass is observed at the end of the cycles at either 50 or 99% RH. In contrast, the moisture
463 content of the samples exposed to 1-week cycles at 50% RH evolves from 5.7% to 4.3%, whereas during
464 the "saturation" cycles, the moisture content evolves between 4.0 and 3.5%. This shows the hysteretic
465 sorption/desorption process with the desorption mechanisms being slower than the sorption mechanisms.
466 Using thermodynamic considerations and simulation, Chen et al. [48] have explained that cellulose-
467 hydrogen bonds are associated with strong energy. Therefore, the cellulose-cellulose hydrogen bonds
468 present in the dry material do not reform at the same % RH and breaks once the material is wet.
469 Regarding the samples exposed to 24-hour cycles, the moisture content for either 50 or 90% RH never
470 reaches those of the "saturation" cycles. At 50% RH, this confirms the transient state of the biocomposite
471 sorption, i.e., the presence of moisture gradients, which potentially induce internal stresses within the
472 biocomposite [12].
473 The samples exposed to 24-hour cycles exhibit moisture contents at the end of the cycles that are constant
474 over more than 100 cycles. At the same time, a decrease in mass is recorded for the 1-week cycles, in a
475 lower magnitude than for the saturation cycles. This shows that the activity of microorganisms (Fig. 4)
476 might be triggered by exposure to the high moisture content and is time-dependent.

3.2.2 Permanent deformations across the "transient" cycles

Fig. 12a, b, and c shows the longitudinal, transversal, and out-of-plane permanent deformations across the cycles for the samples exposed to 24-hour and 1-week "transient" cycles, along with those of the samples exposed to "saturation" cycles between 50 and 99% RH. As for the "saturation" cycles, no permanent deformation occurs in longitudinal or transversal directions across the "transient" cycles.

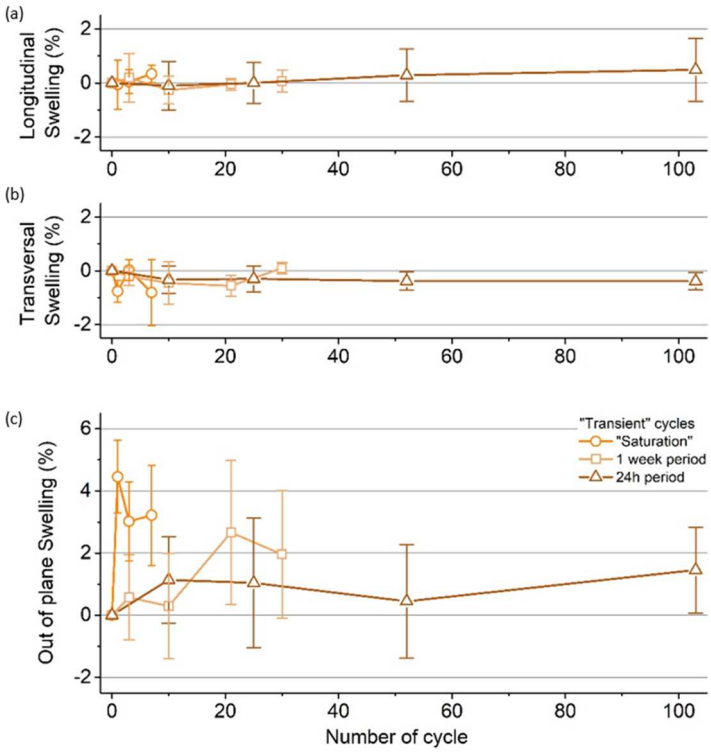

Fig. 12 – Permanent swelling in the longitudinal (a), transversal (b), and out-of-plane (c) directions of flax/PP+MAPP biocomposite unidirectional samples across different "transient" cycles

In the out-of-plane direction, "saturation" cycles induce around 3% permanent deformation against around 2% for 1-week cycles and between 1.5 and 2% for 24-hour cycles. This confirms that the "transient" cycles may be less damaging than the "saturation" cycles and that the cycling methodology is important to qualify the durability of biocomposites. Moreover, permanent deformations, related stress states, and potential damage are observed in the out-of-plane direction, regardless of the type of hygroscopic cycles tested. This is due to the development of internal damage, such as cracks at fibre bundle/matrix and single fibre/single fibre interfaces within the bundles (Fig. 6). This is, therefore, a key mechanism that contributes to the durability of biocomposites against hygroscopic cycles.

494 Nonetheless, it needs to be kept in mind that permanent deformations are measured throughout the whole
495 thickness, which gives an overall picture of the damage to the materials. During the "transient" cycles,
496 materials are submitted to local moisture content gradients that induce internal stresses even in the core of
497 the material. The localisation of the damage is not observable in the present case.
498 As explained in section 3.1.2, the increase of out-of-plane permanent deformations is linked to an
499 increase of the material volume, reduction of density, and thus porosity content. The samples exposed to
500 24-hour cycles are subjected to these phenomena in a lower order of magnitude than those exposed to 1-
501 week cycles.

502 *3.2.3 Longitudinal and transversal stiffness across the "transient" cycles*
503 After exposition to "transient" cycles, biocomposites all show a typical non-linear behaviour in
504 longitudinal directions that is not altered by cycling (not shown here). Fig. 13a and b shows the evolution
505 of the longitudinal and transversal stiffnesses of the flax/PP+MAPP samples measured at stabilization at
506 23°C, 50% RH on unidirectional tensile samples that were previously exposed to different "transient"
507 hygroscopic cycles. "Saturation" results from the hygroscopic cycles between 50 and 99% RH are
508 presented for comparison.
509 The longitudinal stiffness exhibits a drop of about 20% within 100 cycles for the 24-hour duration and the
510 30 cycles of 1-week duration. "Saturation" cycles lead to a more significant decrease in longitudinal
511 stiffness, with 32% along the seven cycles. A drop of 55% of transversal stiffness is observed within 30
512 1-week cycles vs. 27% within 100 24-hour cycles. For saturation cycles, the decrease in transversal
513 stiffness is in the same order of magnitude as that of the samples exposed to 1-week cycles. However, it is
514 reached after a fewer number of cycles.
515

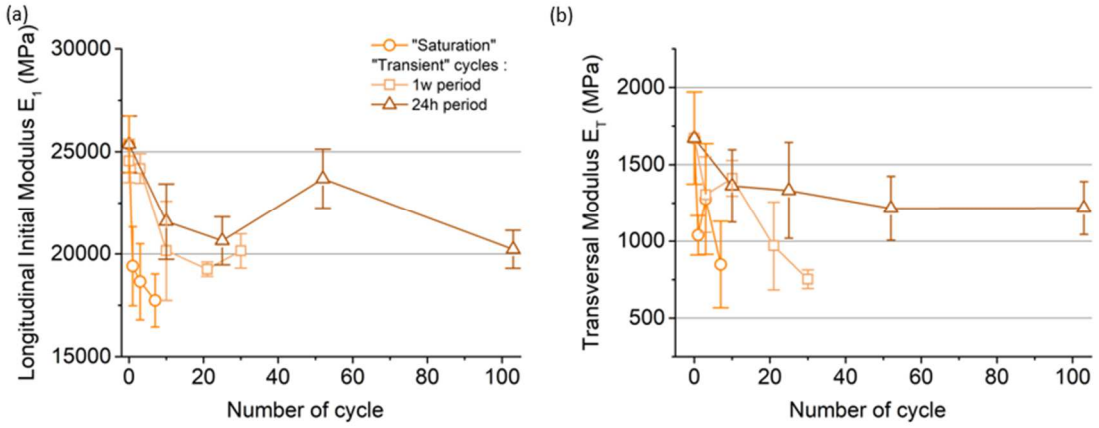

516

517 **Fig. 13 – a) Longitudinal stiffness E_1 and b) transversal stiffness E_T of the flax/PP+MAPP unidirectional**
518 **biocomposites measured at 23°C, 50% RH, after exposition to the "transient" hygroscopic cycles.**

519

520 The duration of the cycles, the moisture sorption reached, and the time spent at high moisture contents are
521 key parameters to the process of damaging biocomposite samples and lowering their mechanical
522 properties.

523 *3.2.4 Curvature across the "transient" cycles and approximation of the internal stresses reached*

524

525 Fig. 14 shows the curvature at the end of cycles for the different cycling conditions of the flax/PP+MAPP
526 asymmetric samples exposed to "transient" hygroscopic cycles. Regarding the curvature across the 24-
527 hour cycles and the curvature at 99% RH at the end of the 1-week cycles, a slight decrease is recorded.

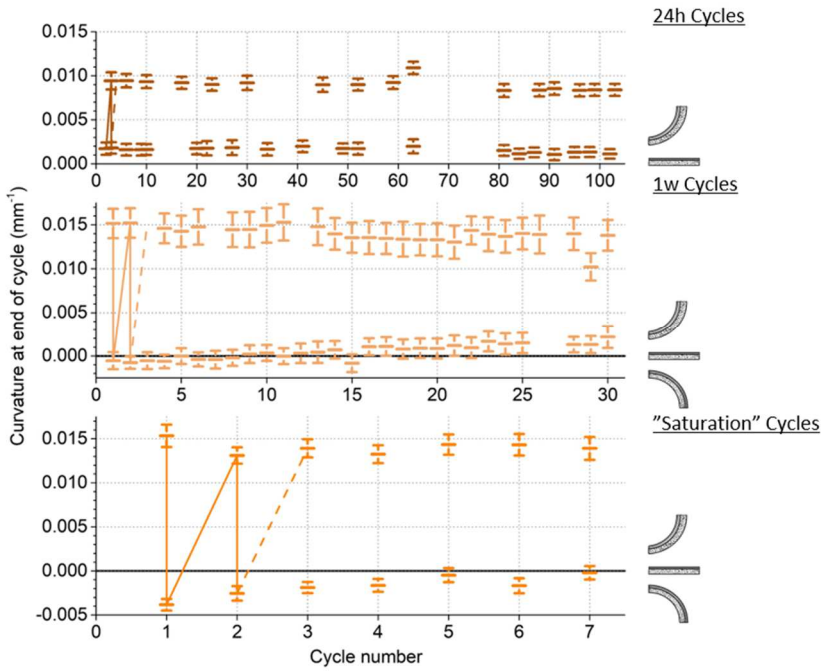

528

529 **Fig. 14 – Curvatures at stabilization of the flax/PP+MAPP asymmetric biocomposite samples across the**
530 **"transient" hygroscopic cycles.**

531

532 As previously done, transversal internal stresses are approximated during the hygroscopic cycles by
533 keeping a constant variation of stiffness with moisture. Only the evolution of the stiffness with the
534 number of cycles is taken into account. It should be kept in mind that another approximation is made here
535 that the internal hygroscopic stresses are homogeneous across the composite thickness. The results of
536 these calculations are presented in Fig. 15.

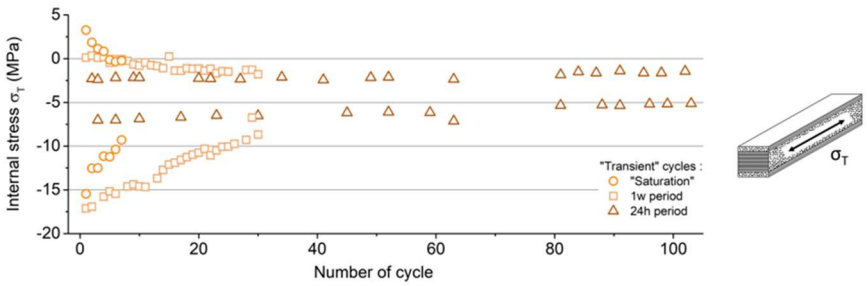

537

538 **Fig. 15 – Curvatures at stabilization of the flax/PP+MAPP asymmetric biocomposite samples across the**
539 **"transient" hygroscopic cycles.**

540

541 Even though the samples exposed to 24-hour cycles are periodically exposed to 90% RH, the reduction of
542 their internal stresses is low compared to longer cycling periods. Approximated compressive stress

543 decreases from -7.0 to $-5.1\ MPa$ after 100 cycles at 90% RH, and from -2.3 to $-1.4\ MPa$ at 50% RH.
544 In addition, the overshoot of curvature observed for the "saturation" cycles between 99 and 50% RH is
545 not observed on the 24-hour nor on the 1-week cycles.
546 Relaxation is a time-dependent mechanism where visco-plastic flows of polymers are triggered. This is
547 confirmed by the fact that five 1-week cycles are required for the stress state to reach the magnitude
548 recorded during the first "saturation" cycle. This shows that the evolution of internal stresses depends not
549 only on the magnitude of moisture content reached but also on the time spent at high moisture contents.
550 This could be due to the viscoelastic behaviour and, therefore, the stress relaxation of the matrix and the
551 mechano-sorptive behaviour of the fibre [49]. In the framework of an outdoor application, 24-hour cycles
552 may be more representative of the lifetime of a biocomposite part as humidity varies from sunrise to
553 sunset. "Saturation" cycles are thus extremely damaging. Interestingly, the flax/PP+MAPP biocomposites
554 examined in this study are quite resistant to dry cycles and to wet cycles with low cycling periods.
555 Nevertheless, the decrease in mechanical properties is linked to the relaxation of the internal stresses,
556 which might be interesting in certain applications, such as when deformation induced by internal stresses
557 is a drawback.
558 Based on the results shown in the paper, Fig. 16 proposes a global scenario representing the stress state
559 evolution within the biocomposites examined.

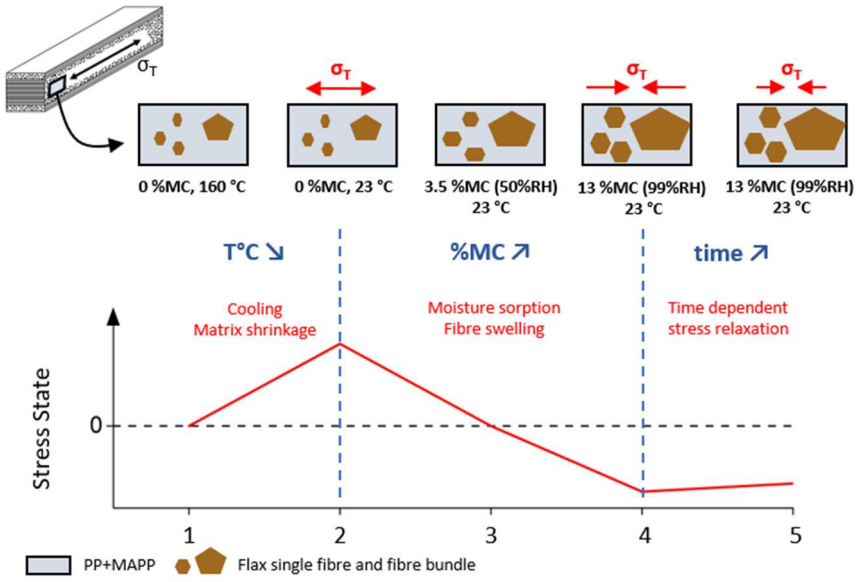

560

561 **Fig. 16 – Development of the stress state within the flax/PP+MAPP biocomposite. Step 1 is the solidification**
562 **of the matrix. Step 2 is the demoulding of the part, Steps 3 to 5 are several steps of the moisture sorption of the**
563 **biocomposite part.**

4. Conclusion

Natural fibre-reinforced biocomposite materials are sensitive to moisture variation and contribute to the development of hygroscopic internal stresses. They have also been shown to be sensitive to the hygroscopic cycling that is found in a wide range of outdoor applications. However, scant attention has been paid in the literature to the evolution of internal stresses during cycles and their contribution to the degradation of their overall properties.

The purpose of this article was to provide deeper insights regarding the development and evolution of hygroscopic stresses within flax/PP+MAPP biocomposites during different hygroscopic cycles. Cycling conditions such as cycling time from transient to saturation state and cycling RH boundaries were evaluated. “Saturation” cycles, where the stabilization in mass triggered the change in condition, were achieved at 23°C, between 11 and 50% RH, 50 and 99% RH, and between 11 and 99% RH. “Transient” cycles with fixed periods were also used: 1-week cycles from 50 to 99% RH, and 24-hour cycles from 50 to 90% RH. The moisture content and curvature of asymmetric stripes and the deformations and stiffness of unidirectional longitudinal and transversal tensile samples were examined throughout various hygroscopic cycles.

Several phenomena, enhanced with the time spent at high moisture contents, were observed, leading to the proposal of a degradation scenario:

- Loss in dry mass along the cycles, possibly due to the activation of the activity of microorganisms;
- Permanent deformations in the out-of-plane direction, and thus increase in void content;
- Loss in longitudinal and transversal stiffness;
- Internal hygroscopic stresses higher than transverse strength of the biocomposites, which induced damages at the fibre/matrix interface;
- Reduction of these internal stresses along cycles due to damage development and time-dependent relaxation mechanisms (viscous flowing of the matrix, mechanosorptive behaviour of fibre).

Credit authorship contribution statement

V Popineau: Investigation and writing; M Peron: review & editing; A Celino: supervision review & editing; C Baley: Supervision, writing - review & editing; A Le Duigou: Supervision, fund acquisition, writing - review & editing.

Declaration of competing interest

The authors declare that they have no known competing financial interests or personal relationships.

Acknowledgement

This work was supported by the Région Bretagne, the Département of Morbihan (France). The authors wish to thank Nicole Geslin for post-editing the English style.

References

[1] Gager V, Le Duigou A, Bourmaud A, Pierre F, Behlouli K, Baley C. Understanding the effect of moisture variation on the hygromechanical properties of porosity-controlled nonwoven biocomposites. Polymer Testing 2019;78 :105944. https://doi.org/10.1016/j.polymertesting.2019.105944.

[2] Popineau V, Célino A, Le Gall M, Martineau L, Baley C, Le Duigou A. Vacuum-Bag-Only (VBO) Molding of Flax Fiber-reinforced Thermoplastic Composites for Naval Shipyards. Applied Composite Materials 2021. https://doi.org/10.1007/s10443-021-09890-2.

[3] Wambua P, Ivens J, Verpoest I. Natural fibres: can they replace glass in fibre reinforced plastics ? Composites Science and Technology 2003;63:1259–64. https://doi.org/10.1016/S0266-3538(03)00096-4.

[4] Le Duigou A, Davies P, Baley C. Environmental impact analysis of the production of flax fibres to be used as composite material reinforcement. Journal of Biobased Materials and Bioenergy 2011;5:1–13. https://doi.org/10.1166/jbmb.2011.1116.

[5] Hill C, Hughes M. Natural fibre reinforced composites opportunities and challenges. Journal of Biobased Materials and Bioenergy 2010 ;4:148–58. https://doi.org/10.1166/jbmb.2010.1079.

621 [6] Le Duigou A, Merotte J, Bourmaud A, Davies P, Belhouli K, Baley C. Hygroscopic expansion: A
622 key point to describe natural fibre/polymer matrix interface bond strength. Composites Science
623 and Technology 2017;151:228–33. https://doi.org/10.1016/j.compscitech.2017.08.028.
624 [7] Péron M, Célino A, Dine, Castro M, Jacquemin F, Duigou A Le. Study of hygroscopic stresses in
625 asymetric biocomposite laminates. Composites Science and Technology 2019 ;169:7–15.
626 https://doi.org/S0266353818321602.
627 [8] Parlevliet PP, Bersee HEN, Beukers A. Residual stresses in thermoplastic composites - a study of
628 the literature. Part I: Formation of residual stresses. Composites Part A: Applied Science and
629 Manufacturing 2007; 37, 11pp 1847-1857. https://doi.org/10.1016/j.compositesa.2006.12.005.
630 [9] Parlevliet PP, Bersee HEN, Beukers A. Residual stresses in thermoplastic composites - a study of
631 the literature. Part II: Experimental Techniques. Composites Part A: Applied Science and
632 Manufacturing 2007; 38, 3 pp 651-655. https://doi.org/10.1016/j.compositesa.2006.12.005.
633 [10] Parlevliet PP, Bersee HEN, Beukers A. Residual stresses in thermoplastic composites - a study of
634 the literature. Part III: Effects of thermal residual stresses. Composites Part A: Applied Science
635 and Manufacturing 2007; 6pp 1581-1596. https://doi.org/10.1016/j.compositesa.2006.12.005.
636 [11] Péron M, Jacquemin F, Casari P, Orange G, Bikard J, Bailleul J, et al. Measurement and
637 prediction of residual strains and stresses during the cooling of a glass fibre reinforced PA66
638 matrix composite. Composites Part A: Applied Science and Manufacturing 2020.
639 https://doi.org/10.1016/j.compositesa.2020.106039.
640 [12] Péron M, Célino A, Jacquemin F, Le Duigou A. Hygroscopic stresses in asymmetric
641 biocomposite laminates submitted to various relative humidity conditions. Composites Part A:
642 Applied Science and Manufacturing 2020; 134, 2020, 105896
643 https://doi.org/10.1016/j.compositesa.2020.105896.
644 [13] Timoshenko S. Analysis of bi-metal thermostats, J. Opt. Soc. Am,11,1925:233–55.
645 [14] Tacq J. Residual and internal stress development resulting from plastic deformation of multi-
646 phase alloys, doctoral thesis KU leuven (Belgium), 2015
647 [15] Lacoste E. Modélisation et simulation multi-échelles des contraintes d'élaboration et de service
648 dans les matériaux composites, doctoral thesis, University of Nantes (France), 2010.

649 [16] Thomason JL, Yang L, Gentles F. Characterisation of the anisotropic thermoelastic properties of
650 natural fibres for composite reinforcement. Fibers 2017; 5(4), 36.
651 https://doi.org/10.3390/fib5040036.
652 [17] Le Duigou A, Réquilé S, Beaugrand J, Scarpa F, Castro M. Natural fibres actuators for smart bio-
653 inspired hygromorph biocomposites. Smart Materials and Structures 2017;26.
654 https://doi.org/10.1088/1361-665X/aa9410.
655 [18] Célino A, Fréour S, Jacquemin F, Casari P. The hygroscopic behavior of plant fibers: a review.
656 Frontiers in Chemistry 2014;1. https://doi.org/10.3389/fchem.2013.00043.
657 [19] Sar BE, Fréour S, Davies P, Jacquemin F. Coupling moisture diffusion and internal mechanical
658 states in polymers - A thermodynamical approach. European Journal of Mechanics, A/Solids
659 2012;36:38–43. https://doi.org/10.1016/j.euromechsol.2012.02.009.
660 [20] BP Chan, AK. Mohanty and M Misra, Studies on durability of sustainable biobased composites: a
661 review, RSC Adv., 2020, 10, 17955-17999
662 [21] Noor Azwa, B. F. Yousif, A Manalo, WM Karunasena, A review on the degradability of
663 polymeric composites base on natural fibres, 2013 Mater and Des 47:424-442
664 [22] Bailey, J.E., Curtis, P.T., Parvizi, A.: Transverse cracking and longitudinal splitting behavior of
665 glass and carbon-fiber reinforced epoxy cross ply laminates and the effect of poisson and
666 thermally generated strain. Proc. R. Soc. Lond. Ser. A 366(1727), 599–623 (1979)
667 [23] Penn LS, Chou RCT, Wang ASD, Binienda WK. The Effect of Matrix Shrinkage on Damage
668 Accumulation in Composites. Journal of Composite Materials 1988:570–86.
669 [24] Le Duigou A, Castro M. Moisture-induced self-shaping flax-reinforced polypropylene
670 biocomposite actuator. Industrial Crops and Products 2015;71:1–6.
671 https://doi.org/10.1016/j.indcrop.2015.03.077.
672 [25] Le Duigou A, Castro M. Evaluation of force generation mechanisms in natural, passive hydraulic
673 actuators. Nature Publishing Group 2016. https://doi.org/10.1038/srep18105.
674 [26] Le Duigou A, Castro M, Bevan R, Martin N. 3D printing of wood fibre biocomposites: From
675 mechanical to actuation functionality. Materials and Design 2016;96:106–14.
676 https://doi.org/10.1016/j.matdes.2016.02.018.

[27] Le Duigou A, Castro M. Hygromorph BioComposites: Effect of fibre content and interfacial strength on the actuation performances. Industrial Crops and Products 2017;99:142–9. https://doi.org/10.1016/j.indcrop.2017.02.004.

[28] Le Duigou A, Chabaud G, Scarpa F, Castro M. Bioinspired Electro-Thermo-Hygro Reversible Shape-Changing Materials by 4D Printing. Advanced Functional Materials 2019;1903280:1–10. https://doi.org/10.1002/adfm.201903280.

[29] Le Duigou A, Keryvin V, Beaugrand J, Pernes M, Scarpa F, Castro M. Humidity responsive actuation of bioinspired hygromorph biocomposites (HBC) for adaptive structures. Composites Part A: Applied Science and Manufacturing 2019;116:36–45. https://doi.org/10.1016/j.compositesa.2018.10.018.

[30] Gassan J, Bledzki AK. Effect of Cyclic Moisture Absorption Desorption on the Mechanical Properties of Silanized Jute-Epoxy Composites, Polymer Composites, 20, 4, 1999

[31] Kim HJ, Seo DW. Effect of water absorption fatigue on mechanical properties of sisal textile-reinforced composites. International Journal of Fatigue 2006;28:1307–14. https://doi.org/10.1016/j.ijfatigue.2006.02.018.

[32] Newman RH, Thumm A, Clauss EC, Guen MJ Le. Improving Hygrothermal Performance in Epoxy-Biofibre Composites Improving Hygrothermal Performance in Epoxy-Biofibre Composites, Advanced Materials Research. 29-30 (2007) pp 287-2902007. https://doi.org/10.4028/www.scientific.net/AMR.29-30.287.

[33] Newman RH. Auto-accelerative water damage in an epoxy composite reinforced with plain-weave flax fabric. Composites Part A 2009;40:1615–20. https://doi.org/10.1016/j.compositesa.2009.07.010.

[34] Mak K, Fam A. The Effect of Wet-Dry Cycles on Tensile Properties of Unidirectional Flax Fiber Reinforced Polymers. Composites Part B : Engineering, 183, 2020:107645. https://doi.org/10.1016/j.compositesb.2019.107645.

[35] Cadu T, Van Schoors L, Sicot O, Moscardelli S, Divet L. Hygrothermal ageing of flax fibers' bundles and unidirectional flax/ epoxy composite. Are bio-based reinforced composites so sensitive ? Industrial Crops & Products 2019;141:111730. https://doi.org/10.1016/j.indcrop.2019.111730.

[36] Van Schoors L, Cadu T, Moscardelli S, Divet L. Why cyclic hygrothermal ageing modifies the transverse mechanical properties of a unidirectional epoxy-flax fibres composite ? Industrial Ctrop and Products, 164, 2021, 113341, https://doi.org/10.1016/j.indcrop.2021.113341.

[37] Lu MM, Van Vuure AW. Improving moisture durability of fl ax fibre composites by using non-dry fibres. Composites Part A 2019;123:301–9. https://doi.org/10.1016/j.compositesa.2019.05.029.

[38] Khalfallah M, Abbès B, Abbès F, Guo YQ, Marcel V, Duval A, et al. Innovative flax tapes reinforced Acrodur biocomposites : A new alternative for automotive applications. Journal of Materials & Design 2014;64:116–26. https://doi.org/10.1016/j.matdes.2014.07.029.

[39] Baley C, Le Duigou A, Bourmaud A, Davies P. Influence of drying on the mechanical behaviour of flax fibres and their unidirectional composites. Composites Part A: Applied Science and Manufacturing 2012; 43:1226–33. https://doi.org/10.1016/j.compositesa.2012.03.005.

[40] Shah DU. Damage in biocomposites : Stiffness evolution of aligned plant fibre composites during monotonic and cyclic fatigue loading. Composites Part A: Applied Science and Manufacturing 2016;83:160–8. https://doi.org/10.1016/j.compositesa.2015.09.008.

[41] Testoni G.A. In situ long-term durability analysis of biocomposites in the marine environment, doctoral thesis, Ecole Nationale Supérieure des Mines de Paris, 2015. https://pastel.archives-ouvertes.fr/tel-01299806

[42] Le Duigou A, Bourmaud A, Baley C. In-situ evaluation of flax fibre degradation during water ageing. Industrial Crops and Products 2015;70:190–200. https://doi.org/10.1016/j.indcrop.2015.03.049.

[43] Fernandes Diniz JMB, Gil MH, Castro JAAM. Hornification — its origin and interpretation in wood pulps. Wood Science and Technology 2004;37:489–94. https://doi.org/10.1007/s00226-003-0216-2.

[44] S Park, RA.Venditti, HJ ameel, JJ. Pawlak, Changes in pore size distribution during the drying of cellulose fibers as measured by differential scanning calorimetry, Volume 66, Issue 1, 2006, Pages 97-103

[45] Fernando D, Thygesen A, Meyer AS, Daniel G. Elucidating Field Retting Mechanisms of Hemp Fibres for Biocomposites : Effects of Microbial Actions and Interactions on the Cellular Micro-

morphology and Ultrastructure of Hemp Stems and Bast Fibres, BioRes. 14(2), 4047-4084.https://doi.org/10.15376/biores.14.2.4047-4084.

[46] Réquilé S, Le Duigou A, Bourmaud A, Baley C. Deeper insights into the moisture-induced hygroscopic and mechanical properties of hemp reinforced biocomposites. Composites Part A 2019;123:278–85. https://doi.org/10.1016/j.compositesa.2019.05.006.

[47] Holstov A, Farmer G, Bridgens B. Sustainable Materialisation of Responsive Architecture. Sustainability, 9, 435; 2017, https://doi.org/10.3390/su9030435.

[48] Chen M, Coasne B, Guyer R, Derome D, Carmeliet J. Role of hydrogen bonding in hysteresis observed in sorption-induced swelling of soft nanoporous polymers. Nature Communications, 9,3507, 2018, https://doi.org/10.1038/s41467-018-05897-9.

[49] Cissé O, Placet V, Boubakar, L. Mechanosorptive creep in single hemp fibres. Composites week @Leuven and Texcomp-11 Conference, Jan 2013, pp.1 - 7, 2013.<hal-00993418>

5. **Appendix 1**

Linear regressions are calculated from the results presented in Fig. 7a and b, and Fig.13a and b, for the evolutions of the longitudinal and transversal stiffness across the different hygroscopic cycles. The values used in the calculations of the stress states for the longitudinal and transversal stiffnesses E_1 and E_T are respectively calculated with the following equations:

$$E_1 = E_{1.0} + a_L * CY \quad \text{Eq. 5}$$

$$E_T = E_{T.0} + a_T * CY \quad \text{Eq. 6}$$

with CY the number of the cycle at which the stiffnesses are calculated, and $E_{1.0}$, $E_{T.0}$, a_L, and a_T, the parameters of the linear regressions. Those parameters depend on the hygroscopic cycle methodology and are presented in Table 1.

Table 1 - Parameters of the linear regressions for the evolution of longitudinal and transversal stiffnesses across the different hygroscopic cycles

	Longitudinal Stiffness E_1		Transversal Stiffness E_T	
	$E_{1,0}$ (GPa)	a_L (MPa/Cy)	$E_{T,0}$ (GPa)	a_T (MPa/Cy)
Saturation cycles: 11 - 50% RH	23.8	-188	1.73	-55.8
Saturation cycles: 50 - 99% RH	22.6	-824	1.45	-86.7
Saturation cycles: 11 - 99% RH	23.1	-1004	1.44	-121
24-hour cycles 50 - 90% RH	23.3	-27.9	1.49	-3.35
1-week cycles 50 - 99% RH	23.8	-164	1.57	-27.3

764 .